

Evolution of *Tetrahymena* ribozyme mutants with increased structural stability

Feng Guo and Thomas R. Cech

Published online 30 September 2002; doi:10.1038/nsb850

Determining how large RNA molecules stabilize their tertiary structures is critical for understanding how they perform their biological functions. Here we use *in vitro* selection to identify active variants of the *Tetrahymena* ribozyme with increased stability. The mutant pool converged to a single family that shared nine mutations; an RNA representing the consensus sequence was structurally more stable by 10.5 °C and catalytically active at elevated temperatures. Remarkably, of the nine altered sites, most are already known to be involved in tertiary interactions, and the stabilizing mutations primarily improve the packing interactions in the molecular interior. The wild type ribozyme and the selected mutants provide pairs of mesophilic and thermophilic homologs for studying the origin of their thermal stability.

How macromolecules from thermophilic organisms achieve thermostability has been a fascinating question for structural biologists and for the biotechnology industry¹. In protein enzymes, this problem has been investigated extensively by structural comparison of thermophilic and mesophilic homologs and by directed evolution approaches^{2,3}. Thermo-

philic proteins enhance their structural stability through many small structural modifications, using the same set of canonical forces — such as hydrogen bonds, salt bridges and hydrophobic interactions — that are found in all proteins. The stabilizing strategy that each individual protein adopts seems to be largely idiosyncratic.

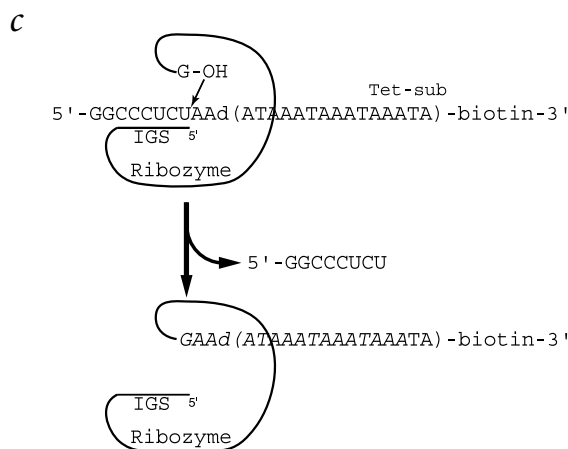
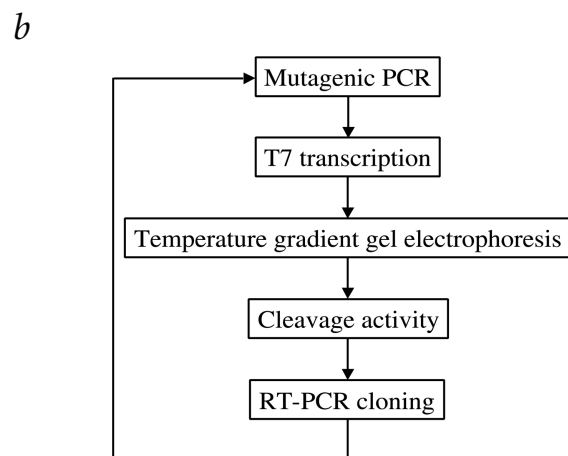
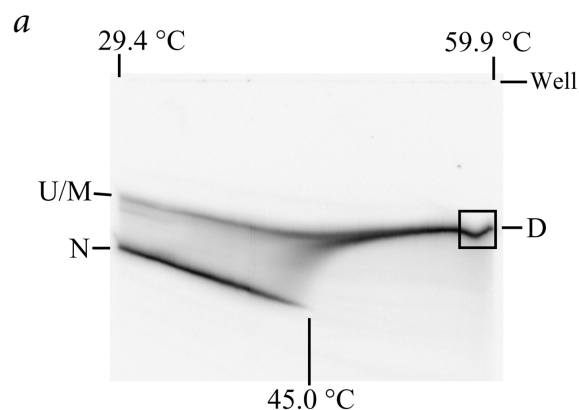


Fig. 1 *In vitro* selection for stability and activity. **a**, A cooperative unfolding transition of the L-21 G414 version of the *Tetrahymena* ribozyme displayed by TGGE in 1× THE and 0.5 mM MgCl₂. A linear temperature gradient was established along the horizontal direction with the temperatures at the ends marked. 'N' stands for native; 'D', denatured (tertiary structure unfolded and secondary structure intact); and 'U/M', unfolded or misfolded. The RNA band in a high-temperature region (boxed) is distorted to variable degrees for unknown reasons. **b**, An *in vitro* selection procedure for thermostable ribozymes. The mutagenic PCR was done at the beginning and again at every third round of selection. **c**, Scheme of the cleavage reaction. The oligonucleotide substrate Tet-sub consists of both ribonucleotides and deoxyribonucleotides (d). An active ribozyme binds to Tet-sub via the internal guide sequence (IGS) and cleaves it using its 3' terminal G residue, which becomes covalently linked to the 3' portion of Tet-sub. The primer-binding site for the subsequent reverse transcription reaction is italicized in the ribozyme-substrate conjugate.

Howard Hughes Medical Institute, Department of Chemistry and Biochemistry, University of Colorado, Boulder, Colorado 80309-0215, USA.

Correspondence should be addressed to T.R.C. email: Thomas.Cech@colorado.edu

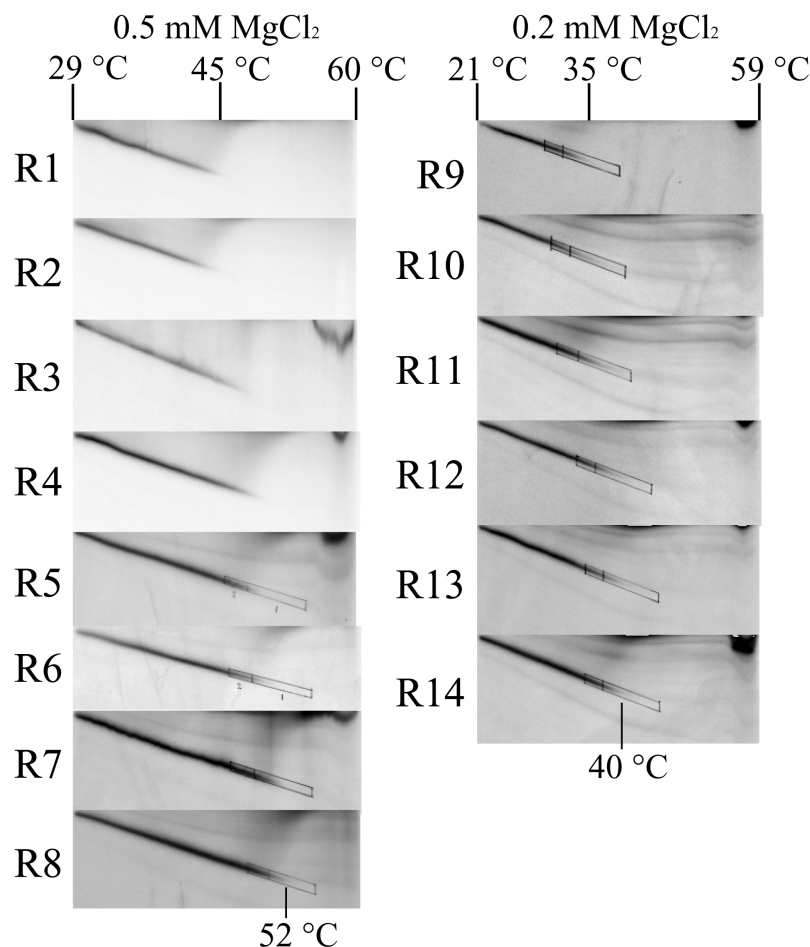


Fig. 2 Selection progression. Portions of TGGE gels of rounds 1–14 (R1–R14) are shown with the $MgCl_2$ concentration and the approximate temperatures across the temperature gradient labeled. These gel pictures are the autoradiograms saved during the selection procedure, except for R1–R4, which are the results using purified RNAs. The right-side boxes on the TGGE gels of R5–R14 represent the regions excised for RNA extraction and subsequent selection procedures.

single-nucleotide bulge deletion that significantly stabilizes the P4–P6 domain of the *Tetrahymena* ribozyme^{14,15}. Because the 160-nucleotide (nt) P4–P6 domain has a relatively simple fold — juxtaposition of two quasi-continuous helices¹⁶ — it remains interesting to see how a larger RNA structure can be stabilized.

We now present a systematic study of thermostability for a catalytic RNA. The 393-nucleotide *Tetrahymena* L-21 G414 ribozyme was chosen mainly because it is the best characterized ribozyme in the self-splicing group I intron family^{16–19}. *In vitro* evolution revealed a robust solution to the problem of making a more stable ribozyme and, at the same time, began to explain some principles that may be general for RNA folding. Specifically, the relatively solvent-inaccessible core (rather than peripheral elements) is not optimized for stability in the natural RNA, and stability can be significantly improved while retaining enzymatic activity.

Similar to protein, RNA can act as an enzyme⁴. However, RNA has a hydrophilic rather than a hydrophobic core, and its structure is formed largely by hydrogen bonding, base stacking and divalent cation-mediated interactions^{5,6}. Thus, the way in which folded RNAs attain thermostability may be different than that of proteins. Increased G+C content and posttranscriptional modifications have been shown to stabilize thermophilic tRNAs^{7–9}. Sequence comparison of the RNase P RNAs from thermophilic bacteria and their mesophilic relatives has revealed several features that may contribute to thermostability¹⁰. For example, the helices in the thermophilic RNAs seem to be stabilized through increased G-C base pairs, minimization of disruptions within helices and/or additional base pairs. Shortened connections between helices were also observed in these thermophilic RNAs. In contrast, a thermodynamic study suggested a mechanism of using a less structured folding intermediate and increased cooperativity rather than increased G+C content to achieve stability for a thermophilic RNase P RNA¹¹. What has been lacking in the field is systematic comparison of homologous large RNA structures with different stability or directed evolution experiments, approaches similar to those used in the studies of protein enzymes.

Although some large ribozyme structures are more thermostable than others^{10–13}, they differ so much in sequence and in their peripheral secondary structure elements that the differences responsible for stability are not easily determined. Thus, *in vitro* selection represents a more feasible approach to explain the basis of structural stability of large RNA molecules. Using a procedure based on native gels, Juneau *et al.* have identified a

Temperature gradient gel electrophoresis (TGGE)

In TGGE, a linear temperature gradient is applied perpendicular to the electric field. Folded RNA molecules become less compact when their tertiary structure is disrupted, with concomitant decrease in electrophoretic mobility. Thus, TGGE allows an entire RNA melting curve to be displayed on a single gel. Previous work established that TGGE could be used to monitor the tertiary-to-secondary structure transition of the 160-nucleotide P4–P6 domain of the *Tetrahymena* ribozyme²⁰. We first searched for a condition in which an enzymatically active form of the *Tetrahymena* ribozyme (L-21 G414, 393 nucleotides) would unfold on TGGE. The native-gel mobility of the ribozyme relative to a 200-base pair (bp) DNA marker remained nearly constant at magnesium concentrations above 1 mM (data not shown), indicative of a folded structure. Eventually, a cooperative unfolding transition of the ribozyme was identified by TGGE at 0.5 mM $MgCl_2$, giving a melting temperature (T_m) of 45 °C (Fig. 1a).

In vitro selection to improve ribozyme thermostability

The strategy for *in vitro* selection (Fig. 1b) used random PCR²¹ mutagenesis of the ribozyme pool at an average level of two mutations per gene, at the beginning and again at every third round of selection. The most stable subpopulation of the initial pool showed a T_m of 45 °C on TGGE, similar to that of the wild type ribozyme (Fig. 2, R1). A gel piece corresponding to extrapolation of the native RNA band was excised (Fig. 2, R5–R14) and the RNA was extracted. The RNA molecules were then selected for activity by requiring them to perform a cleavage-ligation

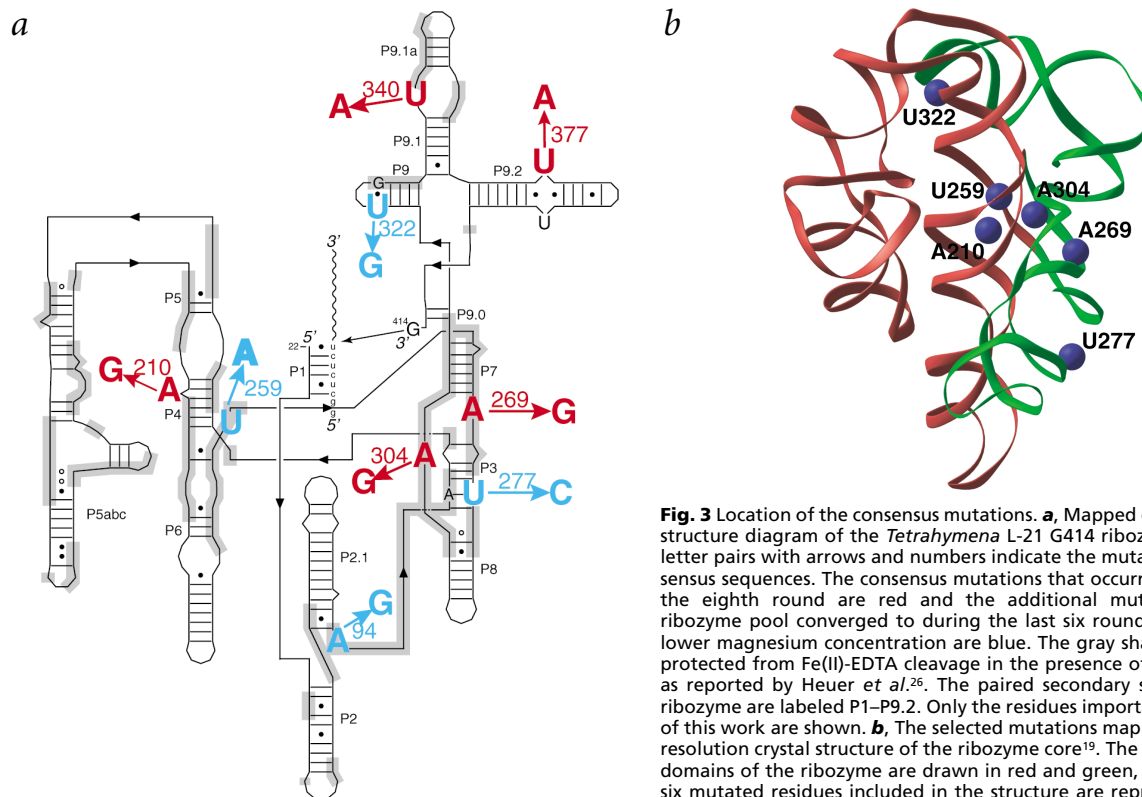


Fig. 3 Location of the consensus mutations. **a**, Mapped on the secondary structure diagram of the *Tetrahymena* L-21 G414 ribozyme. Large bold letter pairs with arrows and numbers indicate the mutations in the consensus sequences. The consensus mutations that occurred at the end of the eighth round are red and the additional mutations that the ribozyme pool converged to during the last six rounds of selection at lower magnesium concentration are blue. The gray shaded regions are protected from Fe(II)-EDTA cleavage in the presence of magnesium ion as reported by Heuer *et al.*²⁶. The paired secondary structures of the ribozyme are labeled P1–P9.2. Only the residues important to the results of this work are shown. **b**, The selected mutations mapped onto the 5 Å resolution crystal structure of the ribozyme core¹⁹. The P4–P6 and P3–P9 domains of the ribozyme are drawn in red and green, respectively. The six mutated residues included in the structure are represented by blue spheres at the C1' atom positions. Peripheral helices P2, P2.1, P9.1 and P9.2 are not present in the structure but were present in the selected ribozyme.

reaction on an added substrate nucleic acid (Fig. 1c); active molecules ligated a primer-binding site to their 3' end, which enabled their amplification by PCR²². During eight rounds of such selection, the apparent T_m of the ribozyme pool gradually increased to ~52 °C.

The unfolding transition of the eighth-round ribozyme pool approached a high-temperature region of the gel where the ribozyme band was distorted to variable degrees for unknown reasons (Figs 1a, 2), making further rounds of selection difficult. Our strategy to overcome this problem takes advantage of the correlation between RNA stability and magnesium ion concentration^{20,23}. Indeed, when the magnesium concentration in TGGE was lowered from 0.5 mM to 0.2 mM, the apparent unfolding transition of the eighth-round pool was shifted from 52 °C to 35 °C. Then six rounds of selection with 0.2 mM MgCl₂ were performed, during which the apparent T_m of the pool at first increased to 40 °C and then failed to improve for the last three rounds (Fig. 2).

The observation that the T_m plateaued in the selection suggests that the ribozyme pool had converged to a common set of mutations and additional mutations failed to further improve the thermostability of the ribozymes. Cloning and sequencing of the survivor ribozymes at the end of the 8th and 14th rounds supported this hypothesis. The eight ribozyme variants sequenced from the 14th round pool contained 9–11 mutations per gene. All of the ribozymes contained a common set of eight mutations, indicating that the pool had indeed converged (Fig. 3a). In addition, one mutation from the group that included U377A, U377G and U376C, which all stabilize the secondary structure of the P9.2 helix, was present in seven vari-

ants. In contrast, the 12 variants from the 8th round pool showed a larger degree of variation, with 5–10 mutations per gene, 5 of which were common to all mutants, including one from the group represented by U377A. The consensus mutations in the 8th round pool (referred to as R8C) were a subset of those in the 14th round pool (referred to as R14C) (Fig. 3a), indicating that R14C was the evolutionary descendant of R8C. Both R8C and R14C were represented by at least one variant sequenced. They were shown in the subsequent characterization to be active for cleavage, and their mutations were sufficient to provide the observed thermostability. The stabilizing mutations identified in the selection are dispersed in the sequence and secondary structure of the ribozyme (Fig. 3a), but are more clustered in the tertiary structure (Fig. 3b).

Structural stability of the selected mutants

The increased thermostability of the 8th and 14th round consensus mutants was confirmed by TGGE (Fig. 4; Table 1). Nevertheless, examining their stability with an independent experimental technique not used in the selection procedure was important. UV melting had been used to monitor the unfolding of the L-21 *ScaI* form of the *Tetrahymena* ribozyme, which lacks five residues at the 3' end of the intron; two major transitions were identified²⁴. Chemical mapping at different temperatures indicated that the first transition primarily involved melting of tertiary interactions and the second involved melting of secondary structures. We found that with 0.4 mM magnesium, thermal unfolding of the wild type *Tetrahymena* L-21 G414 ribozyme gave rise to two transitions with maxima at 58.5 °C and 67.3 °C (Fig. 5). The five mutations in R8C shifted these transitions to

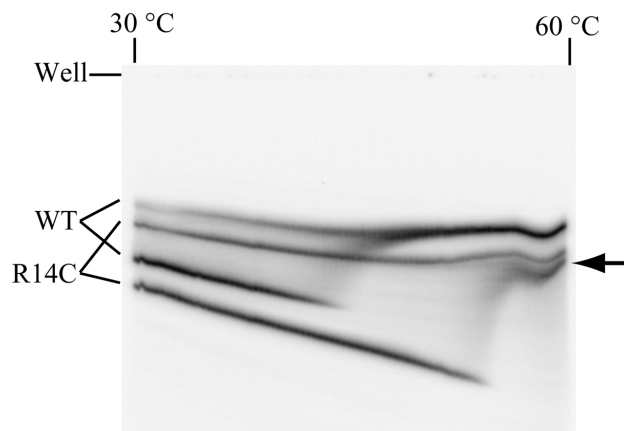


Fig. 4 TGGE comparing R14C with the wild type ribozyme (WT). The electrophoresis was performed in 1× THE buffer and 0.5 mM MgCl₂. The WT RNA was loaded 15 min later than R14C. The assignment of the bands were confirmed by TGGEs with a single RNA sample. The arrow indicates the denatured R14C RNA, which did not converge with the unfolded/misfolded species at high temperature, in contrast to the behavior of the wild type ribozyme.

63.2 °C and 69.5 °C. These temperatures were increased to 65.2 °C and 69.3 °C with R14C. Similar results were observed at 2.0 mM magnesium concentration, with the increases in unfolding transitions smaller than those at 0.4 mM MgCl₂ (data not shown). Assuming that the low-temperature transition primarily monitors the disruption of tertiary interactions for the L-21 G414 ribozyme, these results support the conclusion that the selected mutants possess more stable tertiary structure. In addition, the high-temperature transition, which is generally regarded as a result of the disruption of secondary structure, was also increased by ~2 °C for both mutants. One of the mutations common to R8C and R14C, U377A, closed a U•U mismatch in the P9.2 helix and, thus, could be a primary cause of the elevation of the second-transition temperature. Alternatively, some tertiary structural elements could also contribute to the high-temperature transition and therefore the increase in overall structural stability shifted this transition.

Thermostable activity of the selected ribozymes

Is the structure stabilized by the selected mutations really the catalytically active one? Are the selected mutants active at higher temperature than the wild type? To answer these questions, the single-turnover rate of RNA substrate cleavage reaction was measured at various temperatures for the wild type, R8C and R14C ribozymes (Fig. 6). The wild type ribozyme had a maximum active temperature of 55 °C, whereas the two selected mutants were clearly competent for cleavage at 65 °C (Table 2). Interestingly, the reaction rates of the two mutants seemed to be slower than that of the wild type at 50 or 55 °C. The final extent of reaction of the *Tetrahymena* ribozyme is a function of both the percentage of active ribozymes (ribozymes can be inactive either because they are unfolded or because they are trapped in misfolded conformations) and the equilibrium between cleavage and ligation. We observed that at any given temperature, the final extent of reaction of the stabilized mutants significantly exceeded that of the wild type ribozyme (Table 2).

Interior location of the stabilizing mutations

Overall, the selected mutations do not strengthen the secondary structure of the ribozyme. Only one out of the nine mutations, U377A, stabilizes a helix (P9.2). Two other mutations, U277C and U322G, actually disrupt base pairing in P3 and P9, respectively. Other mutations are located in unpaired regions of the secondary structure (Fig. 3a), many at sites of known tertiary interactions. This is in contrast to an earlier model, derived from a comparison of thermophilic and mesophilic RNase P RNA

sequences¹⁰, that increased use of G-C base pairs and less non-Watson-Crick pairs or mismatches in the secondary structures contribute to thermostability. Therefore, the major improvement in structural stability of the *Tetrahymena* ribozyme seems to originate from introduction or modification of tertiary interactions.

Nucleotides involved in tertiary interactions tend to be conserved among diverse group I introns, or at least constrained in the types of nucleotide substitutions that occur. Searching the Comparative RNA Web Site²⁵, in combination with examining available secondary structural diagrams, revealed that the selected mutations generally follow the phylogenetic trend. For example, A94G and U322G switch nucleotides to the residues that are naturally most abundant in the IC1 and IC2 subgroups (the *Tetrahymena* intron belongs to the IC1 subgroup). Most group I introns do not have a bulged residue in P4 such as that found at position 210 in the *Tetrahymena* intron. However, when there is a bulged residue 210, it occurs as only A or G, with G more abundant; this correlates with the A210G change we observe. This is the same bulged nucleotide that underwent a conformational rearrangement in the previously selected more stable mutant of the isolated P4–P6 domain¹⁵. At position 269, where we observed A269G, A and G residues exist with equal frequency in natural group I introns. A304G mutates from the most abundant residue to the second most abundant one. The P9.1 and P9.2 helices, in which U340A and U377A reside, are not conserved in the group I intron family.

Fe(II)-EDTA protection provides a model-independent method to probe the three-dimensional structures of large RNAs and to distinguish between positions in the interior and exterior of the molecules. When the sites of mutation are superimposed on the Fe(II)-EDTA protection map of the *Tetrahymena* L-21 *ScaI* ribozyme²⁶, four mutated residues are found to be located in the buried region and three others are immediately next to the protected region (Fig. 3a). Therefore, it is largely the relatively solvent-inaccessible core, rather than the peripheral elements, that is not optimized for stability in the natural RNA. The large number of buried sites in the stabilizing mutations is striking compared with the finding in proteins that numerous stabilizing substitutions are found in solvent-exposed areas, as determined by structural comparison of mesophilic and hyperthermophilic proteins and in directed-evolution experiments¹.

Table 1 Melting temperature of ribozymes as determined by TGGE¹

Ribozyme	0.5 mM Mg ²⁺		0.2 mM Mg ²⁺	
	T _m (°C)	ΔT _m (°)	T _m (°C)	ΔT _m (°)
WT	45.0	N.A.	<20 ²	N.A.
R8C	52.5	7.5	33.0	>13
R14C	55.5	10.5	38.0	>18

¹TGGE was carried out in 1× THE buffer and MgCl₂ at indicated concentrations.

²At 0.2 mM magnesium, the wild type ribozyme did not show any native band at the temperature examined.



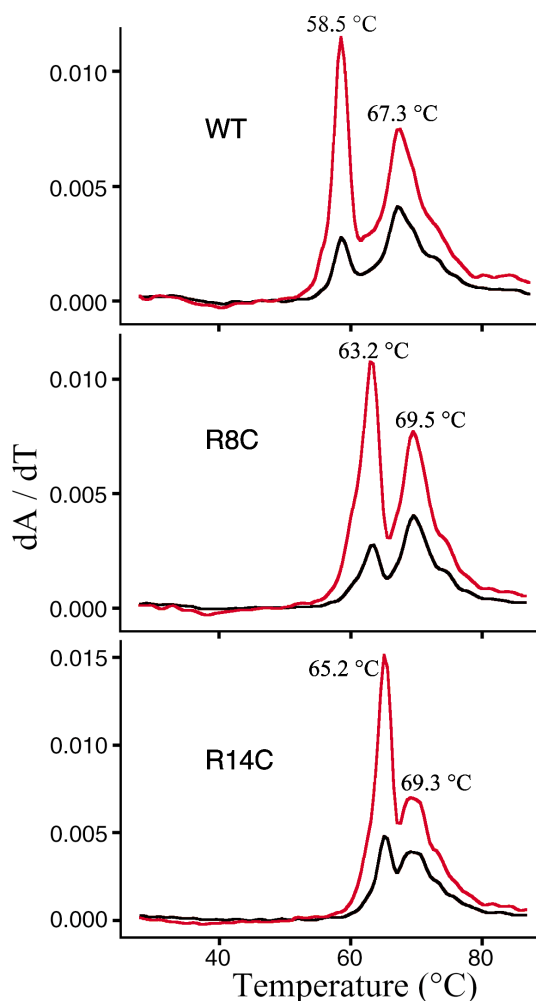
Fig. 5 UV melting of the wild type ribozyme and the consensus mutants. The experiments were performed in 50 mM sodium cacodylate, pH 6.5, and 0.4 mM MgCl₂. The red lines represent the derivative of the absorbance over temperature at 260 nm wavelength and the black lines indicate the absorbance at 280 nm.

Stronger packing interactions in the native state may not be the only mechanism to attain structural stability. A thermodynamic comparison of mesophilic and thermophilic RNase P ribozymes suggested that a less structured intermediate comprises the mechanism to achieve thermostability¹¹. Indeed, the unfolded R14C ribozyme at the high temperature region of TGGE has a slightly different mobility from that of the wild type RNA (Fig. 4), suggesting that our stabilizing mutations also affect the unfolded state.

Mutated sites correspond to known tertiary interactions

The *Tetrahymena* intron is one of the best characterized large ribozyme molecules. The wealth of biochemical and structural data^{16,18,19,27} provides information on molecular properties of the ribozyme mutants, as well as clues to the mechanism of structural stabilization by the selected mutations. The 5 Å resolution crystal structure of the *Tetrahymena* ribozyme core includes six residues that are mutated in R14C¹⁹ (Fig. 3b). Four of these residues, A210, U259, A269 and A304, cluster within relatively short distance, with A269 and A304 the closest. Interestingly, A210, U259 and A304 are located at the interface between the P4–P6 and P3–P9 domains, implying the importance of inter-domain interactions to the overall structural stability of the ribozyme. Nucleotide U277 appears to be external (Fig. 3b) but is thought to be internal in the selected ribozyme, which includes several peripheral helices not present in the P3–P9 molecule that was crystallized.

Nucleotide analog interference mapping (NAIM) is a powerful technique to investigate the importance of the chemical functional groups of ribozymes in catalysis²⁸. In a study on the *Tetrahymena* ribozyme, modification of the backbone 2'-OH group at several of our mutated residues, including A94, A210 and A304, strongly interfered with ribozyme function²⁹. As expected, none of the bases at the mutated sites were shown to be critical. These observations imply that the bases associated with ribose sugars that contribute to critical conformations of large RNA structures are promising candidates to mutate in a search for stable active ribozyme variants.



Michel, Westhof and colleagues^{30,31} proposed models for the *Tetrahymena* ribozyme on the basis of comparative sequence analysis and biochemical data. In their latest model, two mutation sites that are shared by the 8th and 14th round consensus mutants, A304 and A269, interact with each other *via* a *trans* Watson-Crick•Hoogsteen pair. When mutated to Gs, they could form a bifurcated G•G pair, isosteric to the A•A pair in the model. The G•G pair in this configuration can form two bifurcated hydrogen bonds and two water-mediated interactions between the two bases. This pair of mutations could replace the original A•A pair and make the interaction stronger. In 65 secondary structure diagrams of group I introns examined, 16 have Gs at these two positions, the second most abundant following the A•A pair (which appeared 30 times). It is noteworthy that in the highly thermostable self-splicing group I intron in the pre-tRNA^{Ile} of the *Azoarcus* bacterium^{12,13}, both positions are occupied by Gs. Therefore, this pair of mutations could provide a stabilizing interaction to the ribozyme.

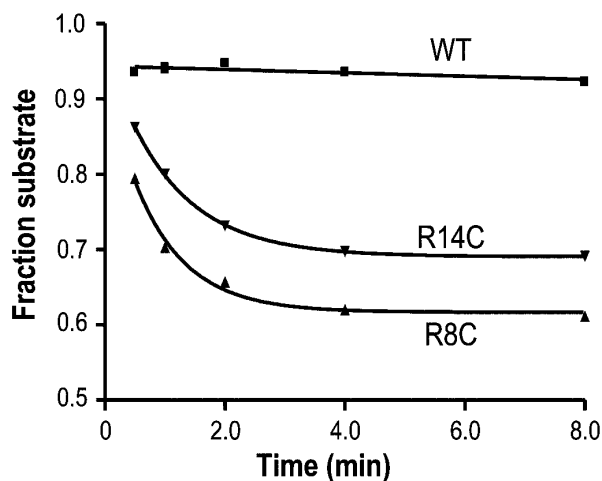


Fig. 6 Selected mutants retain enzymatic activity at high temperature. Single-turnover assays were performed with 5' end-labeled substrate and unlabeled ribozymes at 60 °C (see Methods). The uncleaved substrate as a fraction of the sum of substrate and product bands was fit to an exponential decay function. The reaction rates and final extents of reaction derived from the kinetics of reactions at 40–70 °C are summarized in Table 2.

Table 2 Summary of the substrate cleavage kinetics at various temperatures¹

	40 °C	50 °C	55 °C	60 °C	65 °C	70 °C
WT	0.34 (45) ²	1.99 (36)	1.68 (23)	0 ³	0	0
R8C	0.35 (60)	1.16 (69)	0.95 (51)	1.18 (31)	0.44 (15)	0
R14C	0.47 (75)	0.76 (70)	0.75 (52)	0.94 (28)	0.24 (23)	0

¹The enzymatic system with the L-21 G414 form of the *Tetrahymena* self-splicing intron has been characterized in detail⁴¹. Because of the existence of 3'-terminal G414 residue, the cleavage reaction is reversible and approaches an internal equilibrium.

²The reaction rate (k_{obs} , min⁻¹) and final extent of reaction (%) are shown.

³Ribozyme catalyzed reactions are considered not measurable (marked as 0) when the rate is below 0.01 min⁻¹ or the final extent of reaction is <4%.

In contrast, U259A and U277C each substitute the wild type sequence with a much less abundant residue. Both residues are involved in base-triple interactions as proposed in the literature^{32,33}. These two mutations occurred at low frequency in the eighth round pool and are not included in the R8C consensus. The low magnesium concentration used in the last six rounds of selection may have forced the ribozymes to change the residues that might be otherwise more beneficial to their function at physiological conditions.

Studies on the folding mechanism of the *Tetrahymena* ribozyme have established a hierarchical model involving two domains. The P4–P6 domain is itself an independent folding unit³⁴, whereas the P3–P9 domain is stable only in the presence of a folded P4–P6 at physiological conditions³⁵. In addition, the folding of the P3–P9 domain is the rate-limiting step in the overall folding pathway of the ribozyme^{36,37}. Interestingly, most of our stabilizing mutations are located in the P3–P9 domain, implying that stabilizing the less stable domain is more beneficial than the highly stable P4–P6 domain.

Conclusions

We demonstrated using directed evolution *in vitro* that the thermostability of a natural large ribozyme molecule can be improved. A combination of nine mutations increases the unfolding transition temperature of the *Tetrahymena* L-21 G414 ribozyme by more than 10° in the presence of 0.5 mM Mg²⁺. These mutations strengthen the structure primarily through tertiary interactions, many of which are located in the relatively solvent-inaccessible interior of the RNA fold. The selection results reveal that natural selection did not optimize the stability of this large ribozyme. The wild type ribozyme and the selected mutants comprise pairs of mesophilic and thermophilic homologs with minimal sequence differences, providing an excellent system for further study of the origin of thermal stability.

Methods

RNA preparation. The *Tetrahymena* ribozyme (G22–G414) coding sequence, flanked by a T7 promoter and an *EarI* site, was cloned into a pUC19 plasmid between the *EcoRI* and *XbaI* sites. The ribozymes were transcribed at 37 °C by T7 RNA polymerase and purified using denaturing 4% polyacrylamide gels or a 491 Prep Cell (a tube gel electrophoresis apparatus, BioRad)³⁸. The RNA–DNA chimeric substrate Tet-sub used in the selection and the cleavage kinetics study was synthesized by Dharmacon.

Temperature gradient gel electrophoresis. The experiments were performed essentially as described²⁰. The 1× THE gel running buffer, pH 7.4, contained 34 mM Tris, 66 mM HEPES and 0.1 mM EDTA. MgCl₂ was present at the specified concentration in both the

gel and the running buffer. A total MgCl₂ concentration of 0.5 mM corresponds to ~0.4 mM free Mg²⁺ because of the presence of EDTA. The gel was typically pre-run for 90 min and run for 2 h at 250 V after the sample was loaded.

In vitro selection experiments. Random mutations were introduced into the ribozyme pools at the beginning and at every third round of selection thereafter by mutagenic PCR as described^{21,39}. In the first four rounds of selection, the PCR products containing the ribozyme pool were cloned into a pUC19 plasmid. The ribozyme libraries were transcribed at 37 °C for 3–6 h in 1 ml reactions. The protein was then extracted twice using StrataClean Resin (Stratagene). The RNA solution was concentrated using a Centricon-30 concentrator (Millipore) and buffer-exchanged twice into 1× THE containing 0.5 mM MgCl₂. In rounds 5–14, the PCR products were digested by *EarI* and were used directly as the template for 50 μl T7 transcription reactions containing 40 μCi [α-³²P]CTP and 80 U RNasin ribonuclease inhibitor (Promega). The transcription buffer was exchanged, and unincorporated NTPs were removed using Micro Bio-Spin P-30 columns in 10 mM Tris, pH 7.4 (BioRad). The transcription was normally so clean that no denaturing-gel purification was necessary. The RNA was then annealed by heating to 80 °C for 3 min, cooling to room temperature for 5 min and mixing with an equal volume of a 2× loading buffer containing 2 mM MgCl₂, 10% (w/v) Ficoll 400 (Sigma), 0.08% (w/v) bromophenol blue and 0.08% (w/v) xylene cyanol. The sample was then loaded onto a 6% TGGE gel with MgCl₂ concentrations specified in the text. The RNA bands were visualized by either UV shadow (rounds 1–4) or autoradiography (round 5 and later), and a region determined by extrapolation of the native band to higher temperatures was excised, gel-extracted in TE buffer (10 mM Tris, pH 7.5, and 1 mM EDTA) and ethanol-precipitated. The selected RNA was annealed and subjected to a cleavage reaction containing 50 mM sodium cacodylate, pH 6.0, 5 mM MgCl₂ and 2 μM Tet-sub (Fig. 1c). After incubation at room temperature for 30, 6 or 3 min (for rounds 1–5, 6 and 7–14, respectively), the cleavage reaction was quenched with EDTA, and the RNA was purified using a PCR cleanup kit (Qiagen) eluted in water. A substrate-specific primer and SuperScript II reverse transcriptase (Invitrogen) were used to synthesize cDNA selectively for active ribozyme molecules covalently linked to the 3' portion of Tet-sub (Fig. 1c). The RT product was amplified by PCR using PfuTurbo DNA polymerase (Stratagene). The primers containing the T7 promoter and restriction sites paired with the first 23 and last 27 bases of the *Tetrahymena* L-21 G414 ribozyme gene. The PCR product was used either in the next round of cloning (rounds 1–4) or in T7 transcription.

UV melting. The ribozyme in X mM MgCl₂ was prepared by diluting the RNA in 200 μl of 10 mM sodium cacodylate, pH 6.5, heating to 80 °C for 3 min, cooling to room temperature for 5 min and adding 200 μl of 10 mM sodium cacodylate, pH 6.5, and 2X mM MgCl₂. Then the ribozyme was further diluted to a final concentration of 36 μg ml⁻¹ and a total volume of 1.5 ml in 10 mM sodium cacodylate, pH 6.5, and X mM MgCl₂. The melting curves were measured with a Cary 100 spectrophotometer at both 260 nm and 280 nm wavelengths, from 25 °C to 90 °C with a heating rate of 0.5° min⁻¹. The derivative data were calculated using Thermal (Varian) and smoothed using the Savitzky Golay technique⁴⁰.

Cleavage activity. For the kinetic assays above 50 °C, the cleavage reaction at each time point was performed individually. Ribozyme at 0.5 μM concentration (2 μl) was mixed with 12 μl of 10 mM sodium cacodylate, pH 6.5, and annealed by heating to 80 °C for 3 min, cooling to room temperature for 5 min and adding 2 μl of 10× cleavage buffer containing 400 mM sodium cacodylate, pH 6.5, and 50 mM MgCl₂. The reactions were incubated at the assay temperature for 3 min before being initiated by adding 4 μl of 5' end labeled Tet-sub at ~2.5 nM concentration. To reduce background cleavage resulting from transient exposure to lower temperatures, the Tet-sub solution was incubated at a temperature 10° higher than the assay temperature for at least 3 min before use. The reaction was quenched at reaction temperature by adding 20 μl of 2× splicing stop mix containing 10 M urea, 30 mM EDTA, 0.01% (w/v)



bromophenol blue and 0.025% (w/v) xylene cyanol. The kinetic assays at 40 °C and 50 °C were performed in 100 µl reactions with the same components as described for the higher temperature assays, and the time points were taken by mixing 7 µl reactions with 7 µl 2× splicing stop mix. A 10 µl portion of each sample was loaded onto a denaturing 20% polyacrylamide gel, which was then visualized using an image plate and a Typhoon phosphorimager, and quantitated using ImageQuant (Molecular Dynamics). The substrate data were fit to a one-phase exponential decay curve using PRISM (GraphPad).

Acknowledgements

We are grateful to H. Brummel and K. Kossen for help with the UV melting experiments. We thank A. Gooding for providing T7 RNA polymerase and E. Podell and K. Goodrich for oligonucleotide synthesis. We also thank A. Zaug, A. Berglund, E. Podell, P. Baumann and G. Joyce for insightful discussions.

Competing interests statement

The authors declare that they have no competing financial interests.

Received 12 July, 2002; accepted 4 September, 2002.

- Vieille, C. & Zeikus, G.J. Hyperthermophilic enzymes: sources, uses, and molecular mechanisms for thermostability. *Microbiol. Mol. Biol. Rev.* **65**, 1–43 (2001).
- Petsko, G.A. Structural basis of thermostability in hyperthermophilic proteins, or "there's more than one way to skin a cat". *Methods Enzymol.* **334**, 469–478 (2001).
- Jaenicke, R. & Bohm, G. Thermostability of proteins from *Thermotoga maritima*. *Methods Enzymol.* **334**, 438–469 (2001).
- Doudna, J.A. & Cech, T.R. The chemical repertoire of natural ribozymes. *Nature* **418**, 222–228 (2002).
- Burkard, M.E., Turner, D.H. & Tinoco, I. Jr in *RNA World* (eds Gesteland, R., Cech, T.R. & Atkins, J.) 233–264 (Cold Spring Harbor Laboratory Press, Cold Spring Harbor; 1999).
- Conn, G.L. & Draper, D.E. RNA structure. *Curr. Opin. Struct. Biol.* **8**, 278–285 (1998).
- Watanabe, K., Oshima, T., Iijima, K., Yamaizumi, Z. & Nishimura, S. Purification and thermal stability of several amino acid-specific tRNAs from an extreme thermophile, *Thermus thermophilus* HB8. *J. Biochem.* **87**, 1–13 (1980).
- Kowalak, J.A., Dalluge, J.J., McCloskey, J.A. & Stetter, K.O. The role of posttranscriptional modification in stabilization of transfer RNA from hyperthermophiles. *Biochemistry* **33**, 7869–7876 (1994).
- Galtier, N. & Lobry, J.R. Relationships between genomic G+C content, RNA secondary structures, and optimal growth temperature in prokaryotes. *J. Mol. Evol.* **44**, 632–636 (1997).
- Brown, J.W., Haas, E.S. & Pace, N.R. Characterization of ribonuclease P RNAs from thermophilic bacteria. *Nucleic Acids Res.* **21**, 671–679 (1993).
- Fang, X.W. et al. The thermodynamic origin of the stability of a thermophilic ribozyme. *Proc. Natl. Acad. Sci. USA* **98**, 4355–4360 (2001).
- Reinhold-Hurek, B. & Shub, D.A. Self-splicing introns in tRNA genes of widely divergent bacteria. *Nature* **357**, 173–176 (1992).
- Tanner, M. & Cech, T. Activity and thermostability of the small self-splicing group I intron in the pre-tRNA(Ile) of the purple bacterium *Azoarcus*. *RNA* **2**, 74–83 (1996).
- Juneau, K. & Cech, T.R. *In vitro* selection of RNAs with increased tertiary structure stability. *RNA* **5**, 1119–1129 (1999).
- Juneau, K., Podell, E., Harrington, D.J. & Cech, T.R. Structural basis of the enhanced stability of a mutant ribozyme domain and a detailed view of RNA-solvent interactions. *Structure* **9**, 221–231 (2001).
- Cate, J.H. et al. Crystal structure of a group I ribozyme domain: principles of RNA packing. *Science* **273**, 1678–1685 (1996).
- Cech, T.R. The chemistry of self-splicing RNA and RNA enzymes. *Science* **236**, 1532–1539 (1987).
- Cech, T.R. Self-splicing of group I introns. *Annu. Rev. Biochem.* **59**, 543–568 (1990).
- Golden, B.L., Gooding, A.R., Podell, E.R. & Cech, T.R. A preorganized active site in the crystal structure of the *Tetrahymena* ribozyme. *Science* **282**, 259–264 (1998).
- Szewczak, A.A., Podell, E.R., Bevilacqua, P.C. & Cech, T.R. Thermodynamic stability of the P4-P6 domain RNA tertiary structure measured by temperature gradient gel electrophoresis. *Biochemistry* **37**, 11162–11170 (1998).
- Fromant, M., Blanquet, S. & Plateau, P. Direct random mutagenesis of gene-sized DNA fragments using polymerase chain reaction. *Anal. Biochem.* **224**, 347–353 (1995).
- Beaudry, A.A. & Joyce, G.F. Directed evolution of an RNA enzyme. *Science* **257**, 635–641 (1992).
- Laing, L.G., Gluick, T.C. & Draper, D.E. Stabilization of RNA structure by Mg ions. Specific and non-specific effects. *J. Mol. Biol.* **237**, 577–587 (1994).
- Banerjee, A.R., Jaeger, J.A. & Turner, D.H. Thermal unfolding of a group I ribozyme: the low-temperature transition is primarily disruption of tertiary structure. *Biochemistry* **32**, 153–163 (1993).
- Cannone, J.J. et al. The Comparative RNA Web (CRW) Site: an online database of comparative sequence and structure information for ribosomal, intron, and other RNAs. *BMC Bioinformatics* **3**, 2 (2002).
- Heuer, T.S., Chandry, P.S., Belfort, M., Celander, D.W. & Cech, T.R. Folding of group I introns from bacteriophage T4 involves internalization of the catalytic core. *Proc. Natl. Acad. Sci. USA* **88**, 11105–11109 (1991).
- Couture, S. et al. Mutational analysis of conserved nucleotides in a self-splicing group I intron. *J. Mol. Biol.* **215**, 345–358 (1990).
- Strobel, S.A. & Shetty, K. Defining the chemical groups essential for *Tetrahymena* group I intron function by nucleotide analog interference mapping. *Proc. Natl. Acad. Sci. USA* **94**, 2903–2908 (1997).
- Ortoleva-Donnelly, L., Szewczak, A.A., Gutell, R.R. & Strobel, S.A. The chemical basis of adenosine conservation throughout the *Tetrahymena* ribozyme. *RNA* **4**, 498–519 (1998).
- Michel, F. & Westhof, E. Modelling of the three-dimensional architecture of group I catalytic introns based on comparative sequence analysis. *J. Mol. Biol.* **216**, 585–610 (1990).
- Lehnert, V., Jaeger, L., Michel, F. & Westhof, E. New loop-loop tertiary interactions in self-splicing introns of subgroup IC and ID: a complete 3D model of the *Tetrahymena thermophila* ribozyme. *Chem. Biol.* **3**, 993–1009 (1996).
- Michel, F., Ellington, A.D., Couture, S. & Szostak, J.W. Phylogenetic and genetic evidence for base-triples in the catalytic domain of group I introns. *Nature* **347**, 578–580 (1990).
- Szewczak, A.A. et al. An important base triple anchors the substrate helix recognition surface within the *Tetrahymena* ribozyme active site. *Proc. Natl. Acad. Sci. USA* **96**, 11183–11188 (1999).
- Murphy, F.L. & Cech, T.R. An independently folding domain of RNA tertiary structure within the *Tetrahymena* ribozyme. *Biochemistry* **32**, 5291–5300 (1993).
- Doherty, E.A. & Doudna, J.A. The P4-P6 domain directs higher order folding of the *Tetrahymena* ribozyme core. *Biochemistry* **36**, 3159–3169 (1997).
- Zarrinkar, P.P. & Williamson, J.R. Kinetic intermediates in RNA folding. *Science* **265**, 918–924 (1994).
- Sclavi, B., Sullivan, M., Chance, M.R., Brenowitz, M. & Woodson, S.A. RNA folding at millisecond intervals by synchrotron hydroxyl radical footprinting. *Science* **279**, 1940–1943 (1998).
- Cunningham, L., Kittikamron, K. & Lu, Y. Preparative-scale purification of RNA using an efficient method which combines gel electrophoresis and column chromatography. *Nucleic Acids Res.* **24**, 3647–3648 (1996).
- Guo, F. & Cech, T.R. *In vivo* selection of better self-splicing introns in *Escherichia coli*: the role of the P1 extension helix of the *Tetrahymena* intron. *RNA* **8**, 647–658 (2002).
- Savitzky, A. & Golay, M.J.E. Smoothing and differentiation of data by simplified least squares procedures. *Anal. Chem.* **36**, 1627–1639 (1964).
- Mei, R. & Herschlag, D. Mechanistic investigations of a ribozyme derived from the *Tetrahymena* group I intron: insights into catalysis and the second step of self-splicing. *Biochemistry* **35**, 5796–5809 (1996).